AFORS-HET, A NUMERICAL PC-PROGRAM FOR SIMULATION OF HETEROJUNCTION SOLAR CELLS, VERSION 1.1 (OPEN-SOURCE ON DEMAND), TO BE DISTRIBUTED FOR PUBLIC USE

R.Stangl* (1), A.Froitzheim (2), M.Kriegel (1),
T.Brammer (3), S.Kirste (1), L.Elstner (1), H.Stiebig (3), M.Schmidt(1), W.Fuhs (1)

(1) Hahn-Meitner-Institut Berlin (HMI), Abteilung Silizium Photovoltaik, Kekulé-Str. 5, D-12489 Berlin, Germany
(2) Shell-Solar GmbH, Otto-Hahn Ring 6, D-81739 München, Germany
(3) Photovoltaik-Institut, Forschungszentrum Jülich, D-52452 Jülich, Germany
*Corresponding author: e-mail: stangl@hmi.de, tel: +49/30/8062-1312, fax: +49/30/8062-1333

ABSTRACT: We offer the (new open-source on demand) Version 1.1 of AFORS-HET, a numerical computer simulation program for modeling (thin film) heterojunction solar cells. It will be distributed free of charge on CD-ROM at the conference site and can also be downloaded via internet: www.hmi.de/bereiche/SE/SE1/projects/aSicSi/AFORS-HET
An arbitrary sequence of semiconducting layers can be modeled, specifying the corresponding layer and interface properties, i.e. the defect distribution of states (DOS). Using Shockley-Read-Hall recombination statistics, the one-dimensional semiconductor equations are solved (1) for thermodynamic equilibrium, (2) for steady-state conditions under an external bias and/or illumination, (3) for small additional sinusoidal perturbations of the applied bias/illumination. Thus, the internal cell characteristics, such as band diagrams, local generation and recombination rates, local cell currents, carrier densities and phase shifts can be calculated. Furthermore, a variety of characterization methods can be simulated, such as current-voltage (I-V), internal and external quantum efficiency (IQE, EQE), intensity and voltage dependant surface photovoltage (SPV), photo- and electroluminescence (PEL), impedance spectroscopy (IMP), capacitance-voltage (C-V) and capacitance-temperature (C-T). A user-friendly graphical interface allows not only a visualisation of the simulated data (all data can be imported and exported), but also arbitrary parameter variations can be performed.
Version 1.1 has now been rewritten in a modulized form, such that new measurement methods and new numerical modules can be implemented by external users (open-source on demand). Most measurement methods have been improved and new ones have been added. Several numerical modules have been implemented. The optical generation rate can now be calculated taking into account coherent/incoherent multiple reflections. If modelling crystalline silicon, ionized impurity scattering and carrier-carrier scattering can be considered. The program will be described and demonstrated showing selected results on the simulation of amorphous/crystalline silicon heterojunction solar cells.

Keywords: Simulation, Thin Film, Experimental Methods

1 INTRODUCTION

In order to investigate (thin film) heterojunction solar cells, a lot of different electrical measurement methods are used, ranging from standard solar cell characterisation techniques like current-voltage (I-V) or quantum efficiency (EQE, IQE) to more advanced characterization techniques like for example surface photovoltage (SPV), photo- or electroluminescence (PL, EL), capacitance-voltage (C-V), capacitance-temperature (C-T), impedance (IMP), or intensity modulated photocurrent spectroscopy (IMPS).

We therefore developed a numerical simulation tool (**AFORS-HET**, **a**utomat **for** **s**imulation of **het**ero-structures), which allows to simulate the output of different measurement techniques for an arbitrary sequence of semiconducting layers and interfaces, with an arbitrary number of defects distributed within the different band gaps. A user friendly interface allows to perform multidimensional parameter variations and to visualise and analyse the corresponding results see (Fig.1). Different numerical modules allow to treat different experimental situations, like the choice of a metal/semiconductor or a metal/insulator/semiconductor front contact.

We use the program mainly to simulate amorphous/crystalline silicon heterojunction solar cells, of the structure TCO/a-Si:H(n)/a-Si:H(i)/c-Si(p)/a-Si:H(p^+)/Al, where some ultrathin layers (5 nm) of amorphous hydrogenated silicon are deposited on top of a thick (300 µm) crystalline c-Si(p) wafer.

AFORS-HET is distributed free of charge on CD-ROM and can also be downloaded via internet: www.hmi.de/bereiche/SE/SE1/projects/aSicSi/AFORS-HET. The new version 1.1 of AFORS-HET, which will be launched, is now presented in a modulized form, such that new measurements and new numerical modules can be implemented also by external users (open-source on demand).

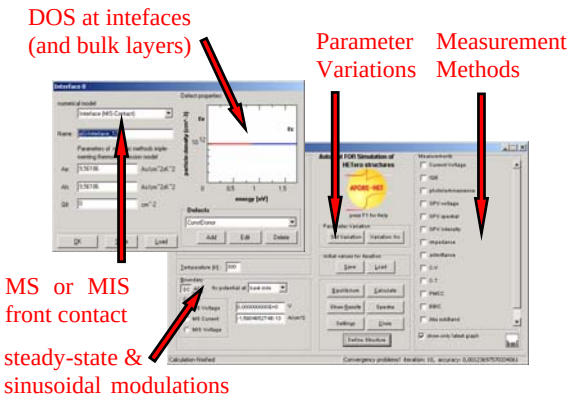

Figure 1: graphical interface of AFORS-HET.

2 MODELLING CAPABILITIES

AFORS-HET numerically solves the one dimensional semiconductor equations with the appropriate boundary conditions under steady-state conditions and under additional small sinusoidal perturbations. The set of coupled partial differential equations is transformed into a set of nonlinear algebraic equations by the method of finite differences. So far, the grid on which the equations are solved is fixed at the beginning of the calculation (fixed x-discretization, non-adaptive meshing), but can be modified by the user, if needed. The free electron density n_i, the free hole density p_i and the cell potential φ_i at each gridpoint are used as independent variables. All other variables in the discretized differential equations / boundary conditions are expressed in a way that they only depend on these independent variables. The resulting nonlinear equations are solved using the Newton-Raphson iteration scheme thereby requiring a good starting solution. If equilibrium conditions are chosen, the program supplies a starting solution from analytical approximations, otherwise the last calculated solution serves as a starting solution for the new boundary conditions to be solved. Alternatively, starting solutions can also be saved and loaded. For more information on the numeric procedure see [1].

With the ability to solve for the internal cell characteristics (band diagrams, local generation and recombination rates, local cell currents, carrier densities and phase shifts) under some specified boundary conditions, measurement methods can be defined by a specific variation of the external boundary conditions and some additional post-processing data analysis.

In the following, the differential equations and corresponding boundary conditions, which are solved by AFORS-HET under various circumstances, are stated. New numerical modules, solving for modified differential equations / boundary conditions may be added by external users (open source on demand).

2.1 Bulk

Poisson's equation and the transport equation for electrons and holes are solved in one dimension.

$$\frac{\varepsilon_0\varepsilon_r}{q}\frac{\partial^2\varphi(x,t)}{\partial x^2} = p(x,t) - n(x,t) + N_D - N_A + \sum_{defects}\rho_t(x,t)$$

$$-\frac{1}{q}\frac{\partial j_n(x,t)}{\partial x} = G_n(x,t) - R_n(x,t) \; - \frac{\partial}{\partial t}n(x,t)$$

$$\frac{1}{q}\frac{\partial j_p(x,t)}{\partial x} = G_p(x,t) - R_p(x,t) \; - \frac{\partial}{\partial t}p(x,t)$$

The electron density n, the hole density p, and the electric potential φ are the independent variables for which the system of differential equations is solved. (q: electron charge, ε_0, ε_r the absolute/relative dielectric constant). $N_{D/A}$ are the concentrations of the donors/acceptors, which are assumed to be completely ionized. The charge stored in the defects is described by a distribution function f_t, specifying the probability that defects with defect density N_t at the position E within the bandgap are occupied with electrons:

acceptor-type defect: $\rho_t(x,t) = -\int dE \; f_t(E,x,t)\,N_t(E)$

donator-type defect: $\rho_t(x,t) = \int dE \; \left(1 - f_t(E,x,t)\right)N_t(E)$

The electron/hole currents $j_{n/p}$ are driven by the gradient of the corresponding quasi Fermi energy $E_{Fn,p}$. Within the bulk of a semiconducting layer, this is equivalent to the sum of a diffusion and a drift current with the corresponding mobility $\mu_{n,p}$.

$$j_n(x,t) = q\mu_n n(x,t)\frac{\partial E_{Fn}(x,t)}{\partial x} = -\frac{\mu_n kT}{q}\frac{\partial n(x,t)}{\partial x} + \mu_n n(x,t)\frac{\partial\varphi(x,t)}{\partial x}$$

$$j_p(x,t) = q\mu_p p(x,t)\frac{\partial E_{Fp}(x,t)}{\partial x} = -\frac{\mu_p kT}{q}\frac{\partial p(x,t)}{\partial x} - \mu_p p(x,t)\frac{\partial\varphi(x,t)}{\partial x}$$

The only time dependence which is treated in this model is a small periodic sinusoidal perturbation of a steady-state condition. That is, neglecting second order terms, all time dependant quantities can be described by a small complex amplitude, i.e.

$$n(x,t) = n(x) + \tilde{n}(x)\,e^{i\omega t} \qquad p(x,t) = p(x) + \tilde{p}(x)\,e^{i\omega t}$$

$$\varphi(x,t) = \varphi(x) + \tilde{\varphi}(x)\,e^{i\omega t}$$

2.1.1 Generation

If the heterostructure is illuminated (specifying the spectral distribution $\Phi(\lambda)$ of the incoming photon flux), the super-bandgap optical generation rate $G_n = G_p$ (for $hc/\lambda \geq E_g$) from the valence band into the conduction band of the semiconductor layers can be obtained in different ways: (1) Assuming simple Lambert-Beer absorption by specifying the spectral absorption coefficient α of each layer. (2) By taking coherent/incoherent internal multiple reflections into account, specifying the dielectric properties (n,k) of each layer. (3) Alternatively, the generation rate can also be imported, using external programs for its calculation. An optical sub-bandgap generation (for $hc/\lambda < E_g$) from a defect to the conduction/valence band can be defined by specifying optical emission coefficients $e_n^o(E)$, $e_p^o(E) \neq 0$ for the defect state:

$$e_n^o(E,x) = \sigma_n^o\, N_C\, \Phi(\lambda,x)\, \vartheta(E_C - E - hc/\lambda)$$

$$e_p^o(E,x) = \sigma_p^o\, N_V\, \Phi(\lambda,x)\, \vartheta(E - E_V - hc/\lambda)$$

($\sigma_{n,p}^o$: optical capture cross sections, $\Phi(\lambda,x)$ spectral photon flux, with wavelength λ at the position x $N_{C,V}$, $E_{C,V}$: conduction/valence band density/energy, ϑ: $\vartheta(E) = 1$ *for* $E \leq 0$, $\vartheta(E) = 0$ *for* $E > 0$)

2.1.2 Recombination

Recombination from the conduction band into the valence band may occur directly (band to band recombination, Auger recombination) and via trap states (Shockley-Read-Hall recombination, SHR):

$$R_{n,p}(x,t) = R_{n,p}^{direct}(x,t) + R_{n,p}^{SHR}(x,t)$$

Direct recombination requires to specify the band to band rate constant r^{BB} and the Auger rate constants r_n^A, r_p^A.

$$R_{n,p}^{direct}(x,t) = R_{n,p}^{direct}(x) + \tilde{R}_{n,p}^{direct}(x)\,e^{i\omega t}$$

$$R_{n,p}^{direct}(x) = \left[r^{BB} + r_n^A n(x) + r_p^A p(x)\right]\left\{n(x)p(x) - N_C N_V e^{-E_g/kT}\right\}$$

$$\tilde{R}_{n,p}^{direct}(x) = \left[r^{BB} + r_n^A n(x)^2 + 2r_p^A n(x)p(x)\right]\tilde{p}(x) + \left[r^{BB} + r_p^A p(x)^2 + 2r_n^A n(x)p(x)\right]\tilde{n}(x)$$

An arbitrary number of defects distributed arbitrarily within the bandgap of the semiconductor layers can be specified. SHR recombination requires to specify the

energetic distribution of the defect density $N_t(E)$ of each defect and its electron/hole capture coefficients $c_{n,p} = v_{n,p}\sigma_{n,p}$ ($v_{n,p}$: thermal velocity, $\sigma_{n,p}$: capture cross section). The emission rates $e_{n,p}$ are then given by

$$e_n(E,x) = c_n N_c\, e^{-(E_c-E)/kT} + e_n^o(E,x)$$
$$e_p(E,x) = c_p N_V\, e^{-(E-E_V)/kT} + e_p^o(E,x)$$

and the SRH recombination rate due to the defects is

$$R_{n,p}^{SRH}(x,t) = R_{n,p}^{SRH}(x) + \tilde{R}_{n,p}^{SRH}(x)\, e^{i\omega t}$$
$$R_n^{SRH}(x) = \int dE\, \{c_n n(x) N_t(E)(1-f_t(E,x)) - e_n(E,x) N_t(E) f_t(E,x)\}$$
$$R_p^{SRH}(x) = \int dE\, \{c_p p(x) N_t(E) f_t(E,x) - e_p(E,x) N_t(E)(1-f_t(E,x))\}$$
$$\tilde{R}_n^{SRH}(x) = \int dE\, \{c_n N_t(E)(1-f_t(E,x))\tilde{n}(x) - c_n N_t(E)\tilde{f}_t(E,x) - e_n(E,x) N_t(E)\tilde{f}_t(E,x)\}$$
$$\tilde{R}_p^{SRH}(x) = \int dE\, \{c_p N_t(E) f_t(E,x)\tilde{p}(x) + c_p N_t(E)\tilde{f}_t(E,x) + e_p(E,x) N_t(E)\tilde{f}_t(E,x)\}$$

The distribution function $f_t(E,x,t)$ describing the occupied defect states is given by SHR theory:

$$f_t(E,x,t) = f_t(E,x) + \tilde{f}_t(E,x)\, e^{i\omega t}$$
$$f_t(E,x) = \frac{c_n n(x) + e_p(E,x)}{c_n n(x) + e_n(E,x) + c_p p(x) + e_p(E,x)}$$
$$\tilde{f}_t(E,x) = \frac{c_n\{1-f_t(E,x)\}\,\tilde{n}(x) - c_p f_t(E,x)\tilde{p}(x)}{c_n n(x) + e_n(E,x) + c_p p(x) + e_p(E,x) + i\omega}$$

2.2 Interfaces

2.2.1 Interface currents driven by drift diffusion

This models uses an interface layer of a certain thickness (which can be specified), in which the material properties change linearly from semiconductor I to semiconductor II. The specified interface defects are distributed homogeneously within this layer. The transport across the heterojunction interface can then be treated like in the bulk of a semiconducting layer (drift/diffusion driven). The cell currents have to be evaluated directly from the gradient of the corresponding quasi fermi energies, since the electron affinity χ, the bandgap E_g and the effective conduction/valence band density of states N_C, N_V will depend on the position x within the interface layer.

$$E_{Fn}(x) = -q\chi(x) + q\varphi(x) - kT\ln\frac{n(x)}{N_C(x)}$$
$$E_{Fp}(x) = -q\chi(x) + q\varphi(x) - E_g(x) + kT\ln\frac{p(x)}{N_V(x)}$$

2.2.2 Interface currents driven by thermionic emission

The transport across a heterojunction interface can alternatively be modeled by thermionic emission over the energetic barrier of the interface, which is the conduction/valence band offset $\Delta E_{C,V}$ (with $\chi^{-,+}, E_g^{-,+}$: electron affinity and bandgap of the semiconductor left or right to the interface):

$$\Delta E_C = q\chi^+ - q\chi^-, \qquad \Delta E_V = E_g^+ - E_g^- + q\chi^+ - q\chi^-$$

The interface is treated as a boundary condition. Thus, conditions for the potential and for the electron/hole currents at both sides of the interface have to be stated ($x_{it}^{-,+}$: position infinitesimal left or right to the interface).

$$\varepsilon_0\varepsilon_r^- \left.\frac{\partial\varphi}{\partial x}\right|_{x_{it}^-} - \varepsilon_0\varepsilon_r^+ \left.\frac{\partial\varphi}{\partial x}\right|_{x_{it}^+} = q\sum_{defects}\rho_{it} \qquad \varphi(x_{it}^-) = \varphi(x_{it}^+)$$

$$j_n(x_{it}^-) = v_n^- n(x_{it}^-)\, e^{-\frac{|\Delta E_C|}{kT}\vartheta(-\Delta E_C)} - v_n^+ n(x_{it}^+)\, e^{-\frac{|\Delta E_C|}{kT}\vartheta(\Delta E_C)} + R_n(x_{it}^-)$$
$$j_n(x_{it}^+) = v_n^+ n(x_{it}^+)\, e^{-\frac{|\Delta E_C|}{kT}\vartheta(-\Delta E_C)} - v_n^+ n(x_{it}^+)\, e^{-\frac{|\Delta E_C|}{kT}\vartheta(\Delta E_C)} - R_n(x_{it}^+)$$
$$j_p(x_{it}^-) = v_p^- n(x_{it}^-)\, e^{-\frac{|\Delta E_V|}{kT}\vartheta(-\Delta E_V)} - v_p^+ n(x_{it}^+)\, e^{-\frac{|\Delta E_V|}{kT}\vartheta(\Delta E_V)} + R_p(x_{it}^-)$$
$$j_p(x_{it}^+) = v_p^+ n(x_{it}^-)\, e^{-\frac{|\Delta E_V|}{kT}\vartheta(-\Delta E_V)} - v_p^+ n(x_{it}^+)\, e^{-\frac{|\Delta E_V|}{kT}\vartheta(\Delta E_V)} - R_p(x_{it}^+)$$

The recombination at the interface is treated equivalently to the bulk recombination, with two exceptions: (1) the interface states are given in cm^{-2} instead of cm^{-3}, (2) the distribution function changes, as the interface states can interact with both adjacent semiconductors:

$$f_{it}(E) = \frac{c_n^+ n(x_{it}^+) + e_p^+(E) + c_n^- n(x_{it}^-) + e_p^-(E)}{c_n^+ n(x_{it}^+) + e_n^+(E) + c_p^+ p(x_{it}^+) + e_p^+(E) + c_n^- n(x_{it}^-) + e_n^-(E) + c_p^- p(x_{it}^-) + e_p^-(E)}$$
$$\tilde{f}_{it}(E) = \frac{c_n^+\{1-f_{it}(E)\}\,\tilde{n}(x_{it}^+) - c_p^+ f_{it}(E)\,\tilde{p}(x_{it}^+) + c_n^-\{1-f_{it}(E)\}\,\tilde{n}(x_{it}^-) - c_p^- f_{it}(E)\,\tilde{p}(x_{it}^-)}{c_n^+ n(x_{it}^+) + e_n^+(E) + c_p^+ p(x_{it}^+) + e_p^+(E) + c_n^- n(x_{it}^-) + e_n^-(E) + c_p^- p(x_{it}^-) + e_p^-(E) + i\omega}$$

2.3 Boundaries

The electric potential is fixed to zero at one contact (for example the back contact). At the second contact a boundary condition has to be specified, which relates the external cell voltage/current to internal quantities. Furthermore, the electron and hole currents into the metal contacts have to be modeled.

2.3.1 Schottky contact, voltage controlled

$$\varphi(0) = \phi_{front} - \phi_{back} + V_{ext} \qquad \varphi(L) = 0$$
$$j_n(0) = qS_n^{front}(n(0) - n_{eq}(0)) \qquad j_n(L) = -qS_n^{back}(n(L) - n_{eq}(L))$$
$$j_p(0) = -qS_p^{front}(p(0) - p_{eq}(0)) \qquad j_p(L) = qS_p^{back}(p(L) - p_{eq}(L))$$

(ϕ: metal work function, S: surface recombination velocity). The majority carrier density under equilibrium (n_{eq} or p_{eq}) is given by the energy barrier of the metal/semiconductor contact, the corresponding minority carrier density (p_{eq} or n_{eq}) by the mass action law

$$n_{eq} = N_c e^{-\frac{q\phi - q\chi}{kT}} \text{ or } p_{eq} = N_V e^{-\frac{E_g - q\phi + q\chi}{kT}}, \quad n_{eq}p_{eq} = N_C N_V e^{-\frac{E_g}{2kT}}$$

2.3.2 Schottky contact, current controlled

The boundary condition for the external cell voltage is replaced by a condition for the external cell current:

$$j_n(0) + j_p(0) = j_{ext}$$

2.3.3 MIS contact, voltage controlled

In case of a metal/insulator/semiconductor front contact, the insulator capacity C_I has to be specified. At x=0 there are additional interface states, which are treated equivalent to the bulk, with the exception that the interface states are given in cm^{-2} instead of cm^{-3}.

$$C_I\{V_{ext} + \varphi(0) - \varphi(L)\} - \varepsilon_0\varepsilon_r^+ \left.\frac{\partial\varphi}{\partial x}\right|_{x=0^+} = q\sum_{defects}\rho_{it} \qquad \varphi(L) = 0$$
$$j_n(0) = 0 \qquad j_n(L) = 0$$
$$j_p(0) = 0 \qquad j_p(L) = 0$$

3 GRAPHICAL INTERFACE

A user-friendly graphical interface allows an easy visualization of all simulated quantities. All data (internal cell results and measurement methods) can be imported and exported and thus graphically compared. The heterostructures and some parts of it (layers, interfaces) can be saved and loaded. The cell dicretization can be modified by the user and also saved and loaded. The same holds for starting solutions used for solving the differential equations. The user can pre-select the measurement methods he wants to use. Arbitrary parameter variations can be performed, selecting an arbitrary number of external and internal input parameter of the program to be varied in a specified range. As an output of a parameter variation, all possible internal cell results as well as measurements can be selected. Parameter variations can also be stored and reloaded.

4 SELECTED RESULTS

In the following section, we like to give a brief overview of the capabilities of the program and highlight its new features. So far, we used the program mainly to simulate amorphous/crystalline silicon heterojuction solar cells in order to study the influence of internal cell parameters on measurements and cell efficiency [2-9].

4.1 Optical calculations

In order to demonstrate the new optical capabilities of the program, Figure 2 shows a comparison with the commercial software window-coating-designer. The reflection and transmission of the mulitlayer stack air/ZnO(80nm)/c-Si(1µm)/air is plotted. Both values are in perfect agreement with the results from window-coating designer. The minimum of R between 500 nm and 600 nm is caused by the TCO with a thickness of 80 nm. The oscillating R and T for a wavelength above 500 nm are interference fringes.

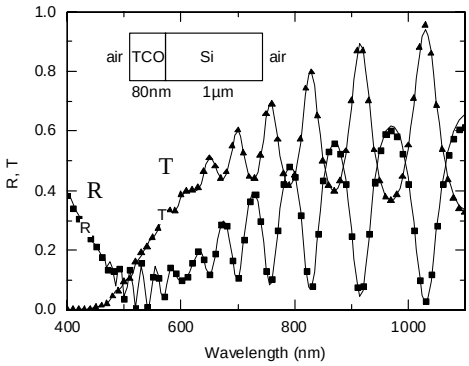

Figure 2: Reflection (R) and transmission (T) of the simple multilayerstack air/ZnO(80nm)/Si(1µm)/air. Comparison of the optical calulations: symbols: AFORS-HET, lines: window-coating designer.

4.2 Internal cell characteristics

The internal cell characteristics, such as band diagrams, local generation and recombination rates, local cell currents, carrier densities and phase shifts can be calculated under various external boundary conditions: I.e., (1) a change of the illumination (variation of wavelength and intensity, choosing an arbitrary spectral illumination file and an additional monochromatic illumination), (2) a change of the external cell voltage (variation of dc-voltage, ac-amplitude and frequency) and (3) a change of the device temperature is possible.

4.3 Simulation of measurement methods

Measurements can be simulated, just by varying external parameters like in a real experiment, and by performing some post-processing data analysis. So far current-voltage (I-V), quantum efficiency (QE), impedance (IMP), capacitance-voltage (C-V), capacitance-temperature (C-T), surface photovoltage (SPV), photo- and electroluminescence (PEL) and electron beam induced current (EBIC) is implemented. New measurement methods may be added by external users (open source on demand).

As an example capacitance-temperature (C-T) simulations are shown, see Fig.3. The capacitance/ conductance at a given frequency ω and an external applied ac-voltage $\tilde{V}_{ext}$ can be calculated from the resulting ac-current $\tilde{j}_{ext}$ through the simulated device:

$$C(\omega) = \frac{1}{\omega} \frac{\mathrm{Im}\{\tilde{j}_{ext}\}(\omega)}{\tilde{V}_{ext}}, \qquad G(\omega) = \frac{\mathrm{Re}\{\tilde{j}_{ext}\}(\omega)}{\tilde{V}_{ext}}$$

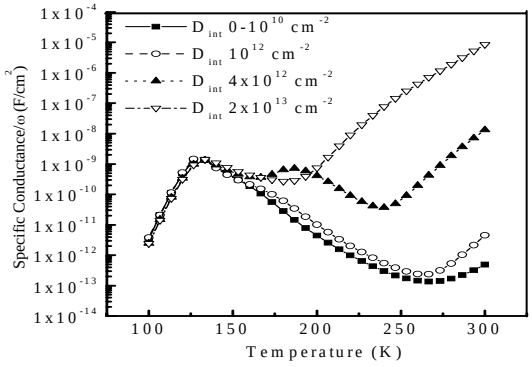

Figure 3: C-T curves at 100 Hz for a-Si:H(n)/c-Si(p) heterostructures simulated with different a-Si:H(n)/ c-Si(p) interface state densities, D_{int} [7].

7 SUMMARY

The capabilities of the simulation program AFORS-HET have been described. The new open-source on demand Version 1.1 will allow external users to implement their own measurement methods and numeric modules. It will be distributed free of charge.

8 REFERENCES

[1] A.Froitzheim, HMI, Dissertation 2003.
[2] Stangl, Froitzheim, Elstner, Fuhs, Proc. 17th Eur. PV Sol. En. Conf., München, Germany 2001, 1387
[3] Froitzheim, Stangl, Elstner Schmidt, Fuhs, Proc. 25th IEEE Conf., New Orleans, 2002
[4] Stangl, Froitzheim, Fuhs., Proc. PV in Europe Conf., Rome, Italy, 2002, 123-126
[5] Froitzheim, Stangl, Kriegel, Elstner, Fuhs, Proc. WCPEC-3, World Conf. PV En. Conv., Osaka, Japan, 2003, 1P-D3-34
[6] Stangl, Froitzheim, Schmidt, Fuhs, Proc. WCPEC-3, World Conf. PV En. Conv., Osaka, Japan, 2003, 4P-A8-45
[7] Gudovskikh, Kleider, Stangl, Schmidt, Fuhs, this conference, 2CV.1.21
[8] Stangl, Schaffarzik, Laades, Kliefoth, Schmidt, Fuhs, this conference, 2CV.1.18
[9] Schmidt, Korte, Kliefoth, Schoepke, Stangl, Laades, Brendel, Scherff, this conference, 2DO.2.5